

# Preparation of complex oxide thin films under hydrothermal and hydrothermal-electrochemical conditions

K. KAJIYOSHI\*, K. YANAGISAWA

*Research Laboratory of Hydrothermal Chemistry, Faculty of Science, Kochi University, 2-5-1, Akebono-cho, Kochi 780-8520, Japan*  
E-mail: kajiyosh@cc.kochi-u.ac.jp

Q. FENG

*Department of Advanced Materials Science, Faculty of Engineering, Kagawa University, 2217-20, Hayashi-cho, Takamatsu 761-0396, Japan*

M. YOSHIMURA

*Center for Materials Design, Materials and Structures Laboratory, Tokyo Institute of Technology, 4259 Nagatsuta, Midori Yokohama 226-8503, Japan*

Thin-film growth of complex oxides including BaTiO<sub>3</sub>, SrTiO<sub>3</sub>, BaZrO<sub>3</sub>, SrZrO<sub>3</sub>, KTaO<sub>3</sub>, and KNbO<sub>3</sub> were studied by the hydrothermal and the hydrothermal-electrochemical methods. Hydrothermal-electrochemical growth of ATiO<sub>3</sub> (A = Ba, Sr) thin films was investigated at temperatures from 100° to 200°C using a three-electrode cell. Current efficiency for the film growth was in the range from ca. 0.6% to 3.0%. Tracer experiments revealed that the ATiO<sub>3</sub> film grows at the film/substrate interface. AZrO<sub>3</sub> (A = Ba, Sr) thin films were also prepared on Zr metal substrates by the hydrothermal-electrochemical method. By applying a potential above ca. +2 V vs. Ag/AgCl to the Zr substrates, AZrO<sub>3</sub> thin films were formed uniformly. KMO<sub>3</sub> (M = Ta, Nb) thin films were prepared on Ta metal substrates by the hydrothermal method. Perovskite-type KTaO<sub>3</sub> thin films were formed in 2.0 M KOH at 300°C. Pyrochlore-type K<sub>2</sub>Ta<sub>2</sub>O<sub>6</sub> thin films were formed at lower temperatures and lower KOH concentrations. Morphotropic phase changes were also revealed in the hydrothermal system KTaO<sub>3</sub>-KNbO<sub>3</sub>.

© 2006 Springer Science + Business Media, Inc.

## 1. Introduction

Synthesis of complex oxide thin films has been extensively investigated mainly because of their electromagnetic properties such as ferroelectricity, piezoelectricity, electro-optic properties, etc. After the initial preparation of BaTiO<sub>3</sub> thin film using flash evaporation in 1955 [1], these oxide thin films have been tried to prepare mainly through dry processes including vacuum evaporation [2], rf and magnetron sputterings [3,4], MOCVD [5], laser deposition [6], and reactive evaporation. In contrast, the hydrothermal and the hydrothermal-electrochemical methods are those novel thin-film formation techniques which make positive use

of hydrothermal and electrochemical reactions between the substrate and species included in the synthesis solution [7–9]. For example, these methods permit a perovskite-type compound ABO<sub>3</sub> to be synthesized on a substrate of B-site metal immersed in a synthesis solution containing A-site ions under hydrothermal conditions. The synthesis temperatures required to obtain crystalline phases in this method are generally below about 300°C, which are fairly lower than the above-mentioned common film-formation techniques. The present paper concerns thin-film growths of complex oxides including BaTiO<sub>3</sub>, SrTiO<sub>3</sub>, BaZrO<sub>3</sub>, SrZrO<sub>3</sub>, KTaO<sub>3</sub>, and KNbO<sub>3</sub> by the hydrothermal and the hydrothermal-electrochemical methods.

\*Author to whom all correspondence should be addressed.

2. Experimental procedure

2.1. Hydrothermal-electrochemical treatments

In case of syntheses of  $\text{ATiO}_3$  ( $A = \text{Ba, Sr}$ ) and  $\text{AZrO}_3$  ( $A = \text{Ba, Sr}$ ) thin films, titanium and Zirconium metal substrates with  $>99\%$  purity and dimensions of  $50 \text{ mm} \times 20 \text{ mm} \times 0.5 \text{ mm}$  were mechanically polished to a mirror finish. A platinum plate with  $\geq 99.0\%$  purity of the same dimensions was also prepared. Prior to the hydrothermal-electrochemical treatment, the Ti substrate and the Pt plate were degreased in acetone with an ultrasonic cleaner, etched in a chromic acid mixture for about 16 h, and then washed in distilled water with the ultrasonic cleaner. Guaranteed grade reagents with  $>98\%$  assay of  $\text{Ba}(\text{OH})_2 \cdot 8\text{H}_2\text{O}$  and  $\text{Sr}(\text{OH})_2 \cdot 8\text{H}_2\text{O}$  was used to prepare  $\text{A}(\text{OH})_2$  ( $A = \text{Ba, Sr}$ ) solutions. Hydrothermal-electrochemical treatments were performed in an autoclave fabricated on the basis of the three-electrode cell arrangement with an  $\text{Ag}/\text{AgCl}$  external reference electrode shown in Fig. 1. A metal substrate and a platinum plate of the same dimensions were suspended as the working and the counter electrodes, respectively, by 0.5-mm-diameter wires of the same metal as the respective electrodes, maintaining a separation of 30 mm between them in the electrolytic cell containing 200–500 mL of a synthesis solution. The temperature profile of the hydrothermal treatment was controlled so that it would follow a heating

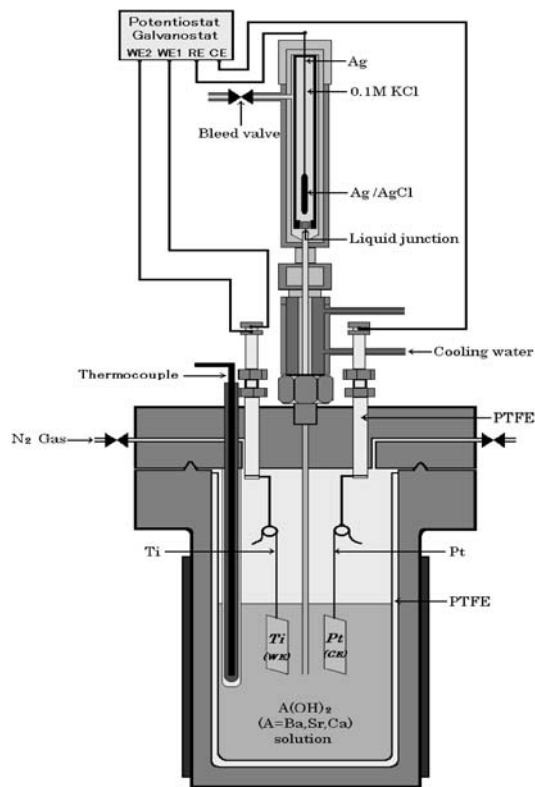


Figure 1 Electrolytic cell of three-electrode arrangement assembled in an autoclave for hydrothermal-electrochemical synthesis.

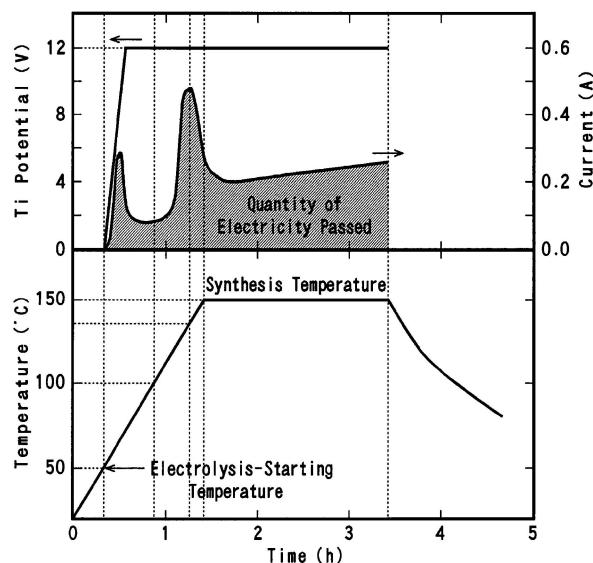


Figure 2 Relation between temperature profile (lower) and potentiostatic electrolysis adopted in the present study (upper). The electrolysis is performed from  $50^\circ\text{C}$  in the heating region to the end of the isothermal region of the temperature profile. The potential of the Ti electrode is represented in units of volts vs.  $\text{Ag}/\text{AgCl}$  electrode. The hatched area below the electrolysis current curve corresponds to the quantity of electricity passed.

region up to a synthesis temperature with a heating rate of  $1.5^\circ\text{C}/\text{min}$ , and a subsequent isothermal region with a soak time. The electrolysis was performed potentiostatically from  $50^\circ\text{C}$  in the heating process to the end of the isothermal process as shown in Fig. 2.

2.2. Hydrothermal treatments

In case of syntheses of  $\text{KMO}_3$  ( $M = \text{Ta, Nb}$ ) thin films, tantalum metal substrates with  $>99.9\%$  purity and dimensions of  $10 \text{ mm} \times 10 \text{ mm} \times 0.5 \text{ mm}$  were mechanically polished. Prior to the hydrothermal treatment, the Ta substrates were washed in  $\text{NaOH}$  solution, degreased in acetone with an ultrasonic cleaner, etched in a chromic acid mixture for about 16 h, and then washed in distilled water with the ultrasonic cleaner. Guaranteed reagent grade  $\text{KOH}$  and  $\text{Nb}_2\text{O}_5$  were used to prepare  $\text{KOH}$  solutions including  $\text{Nb}_2\text{O}_5$ . Hydrothermal treatments at temperatures in the range from  $150^\circ$  to  $400^\circ\text{C}$  were performed in a Hastelloy-C lined microautoclave (Fig. 3) containing 6–10 mL of  $\text{KOH}$  solution and the Ta substrate. In order to investigate the crystal symmetry and the lattice constants of hydrothermally synthesized  $\text{KMO}_3$  ( $M = \text{Ta, Nb}$ ), powder samples were also prepared using guaranteed reagent grade  $\text{Ta}_2\text{O}_5$ ,  $\text{Nb}_2\text{O}_5$ , and  $\text{KOH}$ .

3. Characterization

Film-constituting phases and their lattice parameters were analyzed by X-ray diffractometry (XRD, RINT 1500, Rigaku Denki) under the operating conditions of  $40 \text{ kV}$ - $100 \text{ mA}$ , using  $\text{CuK}\alpha$  radiation with a graphite

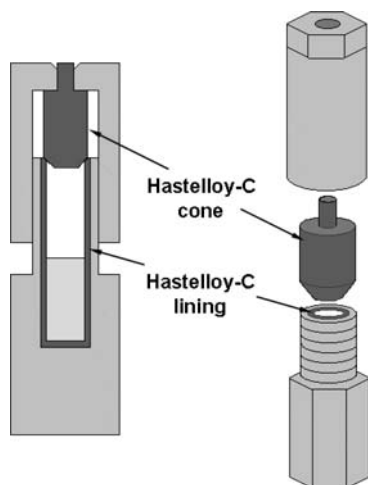


Figure 3 Schematic figure of Hastelloy-C lined autoclave used for hydrothermal synthesis.

monochromator and a silicon powder (Si-640b, U.S. Department of Commerce, NIST). Microstructure of the grown films was investigated using scanning electron microscopy (SEM, S-4000, Hitachi) at an acceleration voltage of 10–20 kV, and by transmission electron microscopy (TEM, H-9000UHR, Hitachi) at an acceleration voltage of 300 kV. Compositional analysis was performed using scanning transmission electron microscopy (STEM, HB501, VG Microscopes) at an acceleration voltage of 100 kV, incorporating energy dispersive X-ray spectroscopy (EDX, KEVEX SUPER8000, Fisons Instruments) with a probe beam of 1-nm diameter and 1-nA current.

Metal/insulator/metal structures were fabricated by depositing an array of 2.0-mm-diameter Ag or Al films on the film surface to measure electrical properties. Leakage current-voltage characteristics and dielectric breakdown voltages were measured with a voltage current source (TR6163, Advantest) and with a picoammeter (TR8641D, Advantest). Dependence of capacitance and dielectric loss on dc bias voltage and temperature was measured with an LCR meter (HP4284A, Hewlett-Packard). Frequency dependence of capacitance and dielectric loss was evaluated with an impedance analyzer (YHP4194A, Yokogawa-Hewlett-Packard). A ferroelectric tester (RT6000HVS, Radiant Technologies) was used to measure polarization-voltage hysteresis loops.

## 4. Results and discussion

### 4.1. Growth of $\text{ATiO}_3$ ( $A = \text{Ba}, \text{Sr}$ ) thin film on titanium substrate by the hydrothermal-electrochemical method

A novel hydrothermal-electrochemical method has been developed to prepare dielectric thin films of  $\text{ATiO}_3$  ( $A = \text{Ba}, \text{Sr}$ ) on Ti substrates with accurate control of the film

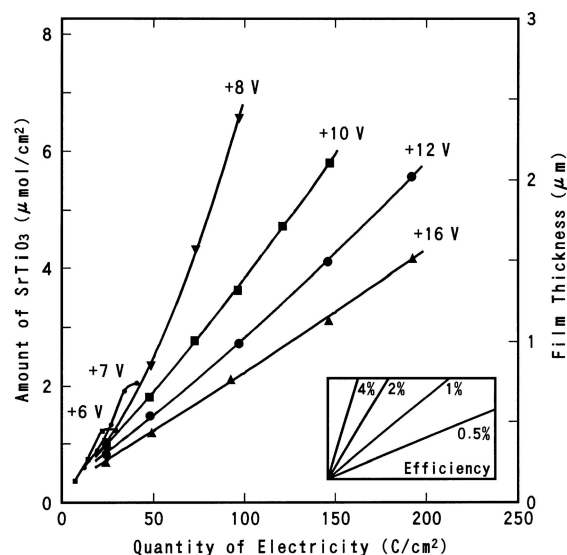


Figure 4 Amount of  $\text{SrTiO}_3$  formed per unit surface area and corresponding film thickness estimated by gravimetry as a function of the quantity of electricity for various Ti electrode potentials (vs. Ag/AgCl). Inset shows slopes corresponding to several typical values of current efficiency.

thickness up to ca.  $2 \mu\text{m}$ . The cubic lattice parameter of the  $\text{SrTiO}_3$  film was analyzed to be  $3.919 \text{ \AA}$ . The film thickness increased monotonically with an increase in the quantity of electricity passed through the Ti electrode, and could be controlled coulometrically by this factor as depicted in Fig. 4. Current efficiency for the film growth was estimated to be in the range from ca. 0.6% to 3.0%, mainly depending on the Ti electrode potential and the synthesis temperature. Solid-solution films in the system  $\text{BaTiO}_3\text{-SrTiO}_3$  were also grown on

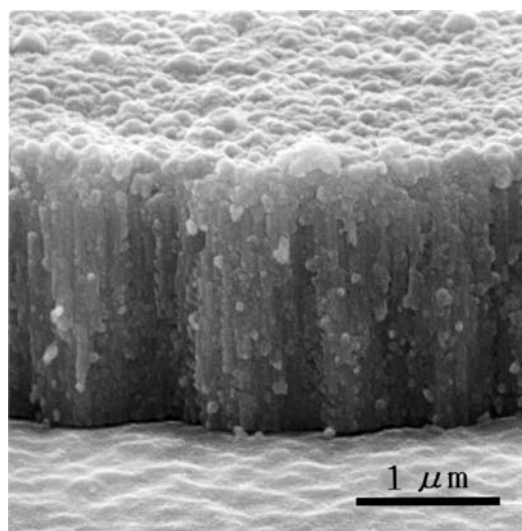


Figure 5 SEM micrograph of a ca.  $2\text{-}\mu\text{m}$ -thick  $\text{SrTiO}_3$  film grown on a Ti substrate by the modified hydrothermal-electrochemical method with potentiostatic electrolysis at  $+8.0 \text{ V}$  vs. Ag/AgCl in  $0.5 \text{ M Sr(OH)}_2$  solution of pH 14.2 at  $150^\circ\text{C}$ .

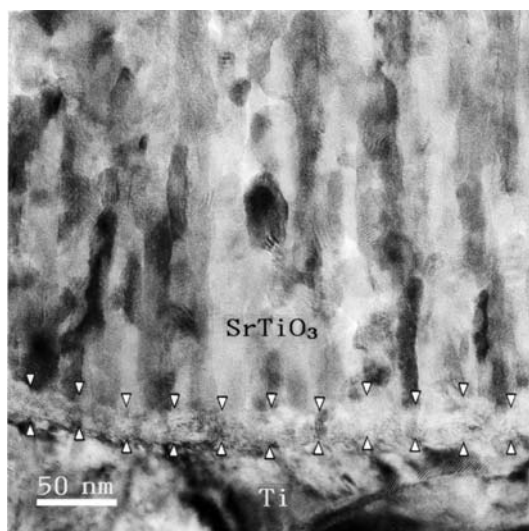


Figure 6 Magnified TEM image of the SrTiO<sub>3</sub> film/Ti substrate interface of the SrTiO<sub>3</sub> film. Arrows indicate boundaries of a polycrystalline layer of Ti oxides whose microstructure is different from the columnar one of the overlying, inner SrTiO<sub>3</sub> layer.

Ti electrodes with control of the Ba/Sr composition in (Ba, Sr)(OH)<sub>2</sub> solutions. The mass transport mechanism during the hydrothermal-electrochemical growth of polycrystalline thin films of ATiO<sub>3</sub> (A = Ba, Sr) perovskite onto Ti electrodes in A(OH)<sub>2</sub> solutions was studied by a tracer technique, using Ba and <sup>18</sup>O atoms as respective tracers for A-site and oxygen atoms in SrTiO<sub>3</sub> host films. It was found that the ATiO<sub>3</sub> film grows at the film/electrode interface by transport of both A-site and oxygen atoms from the solution to the interface. A-site and oxygen atoms are considered to diffuse as constituents of solution species, such as A<sup>2+</sup>, OH<sup>-</sup>, and H<sub>2</sub>O, through open short-circuit paths existing at grain boundaries. Microstructures of SrTiO<sub>3</sub> thin films grown on Ti substrates by the hydrothermal-electrochemical method were studied by scanning and transmission electron microscopy.

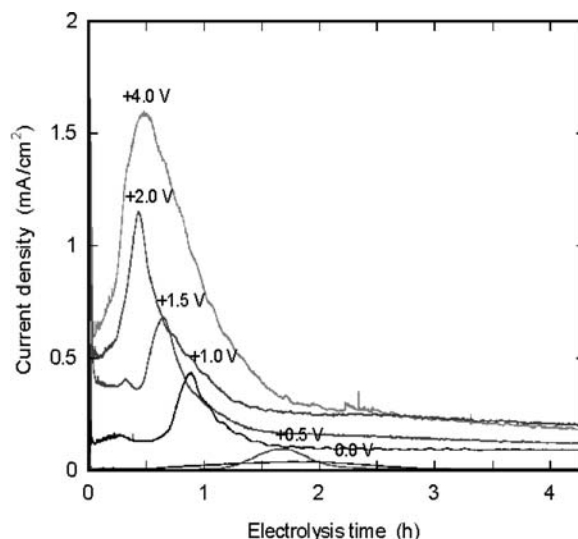


Figure 7 Variation of current density curve with Zr electrode potential (V vs. Ag/AgCl). Synthesis conditions: 0.5 M Ba(OH)<sub>2</sub>, 150°C, 4 h.

The grown films consisted of a thin surface layer having an isotropic polycrystalline structure and a thick inner layer having a columnar structure (Fig. 5). Pores of the order of several tens of nanometers were found at boundaries of columnar grains constituting the inner layer. A 20- or 30-nm-thick polycrystalline layer of Ti oxides contaminated with a small amount of Sr was also found at the SrTiO<sub>3</sub> film/Ti substrate interface (Fig. 6). During the film growth at this interface, the observed pores are considered to act as short-circuit paths for mass transport from the film surface to the interface. Electrical measurements were performed on BaTiO<sub>3</sub> thin films grown by the hydrothermal-electrochemical method. Resistivities as high as 10<sup>12</sup> Ω·cm were obtained in the voltage range up to 2 V for the 0.40-μm-thick BaTiO<sub>3</sub> thin film and its breakdown voltage was higher than 12 V. The grown films were paraelectric with dielectric constants of

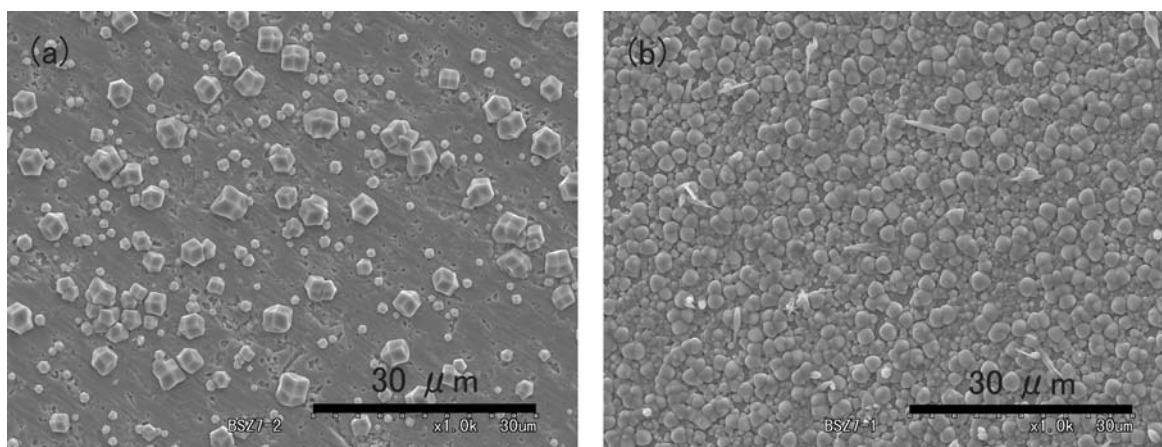


Figure 8 SEM images of (Ba, Sr)ZrO<sub>3</sub> microcrystals formed under (a) hydrothermal and (b) hydrothermal-electrochemical conditions. Synthesis conditions: 0.5 M (Ba<sub>0.5</sub>Sr<sub>0.5</sub>)(OH)<sub>2</sub>, +8.0 V vs. Ag/AgCl, 150°C, 4 h.

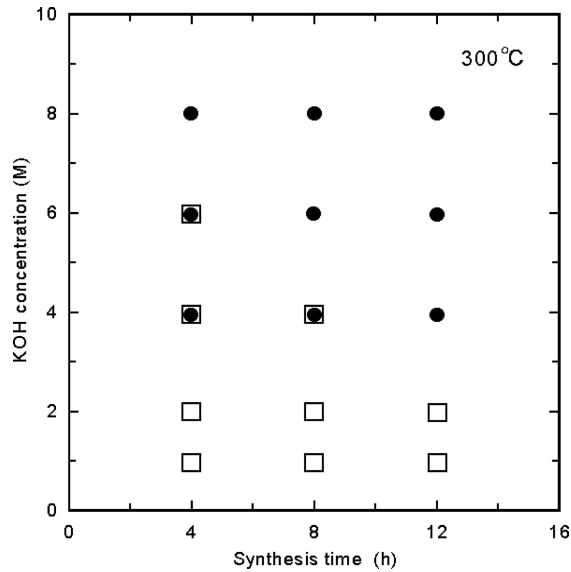


Figure 9 Formation diagram of  $\text{KTaO}_3$  perovskite and  $\text{K}_2\text{Ta}_2\text{O}_6$  pyrochlore in the hydrothermal system  $\text{KOH-Ta-H}_2\text{O}$  at a synthesis temperature of  $300^\circ\text{C}$ . ●:  $\text{KTaO}_3$ , □:  $\text{K}_2\text{Ta}_2\text{O}_6$ .

340–350 and dielectric losses of 7%–10% at 1 kHz, 0.1 Vrms, and  $25^\circ\text{C}$ .

#### 4.2. Growth of $\text{AZrO}_3$ ( $A = \text{Ba}, \text{Sr}$ ) thin film on zirconium substrate by the hydrothermal-electrochemical method

Thin films of  $\text{AZrO}_3$  were prepared on Zr metal substrates by the hydrothermal-electrochemical method [16]. The electrolysis current flowed through the Zr substrate and the resulting surface morphology of grown film largely depended on the electrode potential applied to the substrate, as shown in Figs. 7 and 8. Under pure hydrothermal conditions,  $\text{AZrO}_3$  microcrystals with diameters of several micrometers were formed sparsely on the Zr substrates. By applying a potential above ca. +2 V vs.  $\text{Ag/AgCl}$  to the Zr substrates,  $\text{AZrO}_3$  thin films could be synthesized on them uniformly. Solid-solution films in the system  $\text{BaZrO}_3\text{-SrZrO}_3$  were also grown on Zr substrates with control of the Ba/Sr composition in  $(\text{Ba}, \text{Sr})(\text{OH})_2$  solutions. Thus the electrochemical treatment was confirmed to be effective for fabricating  $\text{AZrO}_3$  thin films, similarly as for  $\text{ATiO}_3$  thin films.

#### 4.3. Growth of $\text{KMO}_3$ ( $M = \text{Ta}, \text{Nb}$ ) thin film on tantalum substrate by the hydrothermal method

Thin films of  $\text{KMO}_3$  were prepared on Ta metal substrates by the hydrothermal method [17]. Fig. 9 shows a phase formation diagram in the hydrothermal system  $\text{KOH-Ta-H}_2\text{O}$  at a synthesis temperature of  $300^\circ\text{C}$ . Phase-pure perovskite-type  $\text{KTaO}_3$  thin films were formed in

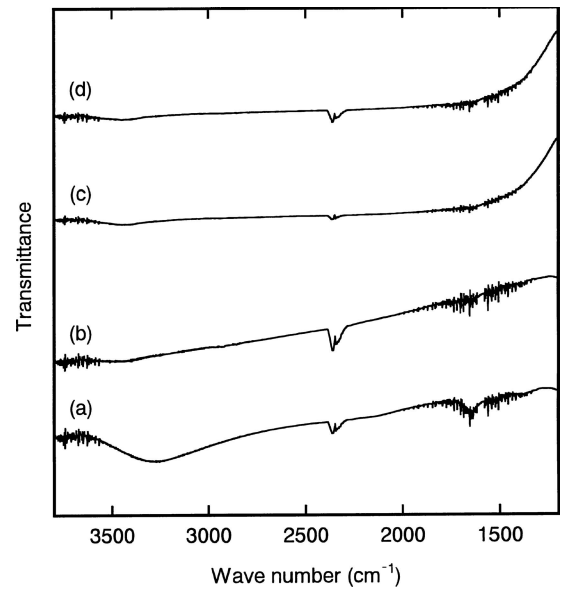


Figure 10 IR spectra of  $\text{KTaO}_3$  and  $\text{K}_2\text{Ta}_2\text{O}_6$  with/without heating at  $1000^\circ\text{C}$  for 4 h in air. (a)  $\text{K}_2\text{Ta}_2\text{O}_6$  as grown, (b)  $\text{K}_2\text{Ta}_2\text{O}_6$  with heating, (c)  $\text{KTaO}_3$  as grown, (d)  $\text{KTaO}_3$  with heating. Synthesis conditions: 8.0 M  $\text{KOH}$ ,  $200^\circ\text{--}300^\circ\text{C}$ , 12 h.

2.0 M  $\text{KOH}$  at  $300^\circ\text{C}$ . Pyrochlore-type  $\text{K}_2\text{Ta}_2\text{O}_6$  thin films were formed at lower temperatures and lower  $\text{KOH}$  concentrations. Lattice constant of the  $\text{KTaO}_3$  was nearly the same as that in JCPDS-PDF, whereas lattice constant of  $\text{K}_2\text{Ta}_2\text{O}_6$  was 0.2% larger than the PDF value. It was found by TG and IR measurements that the  $\text{K}_2\text{Ta}_2\text{O}_6$  pyrochlore contains several percent of OH group whereas the  $\text{KTaO}_3$  perovskite contains only a smaller amount of OH group.

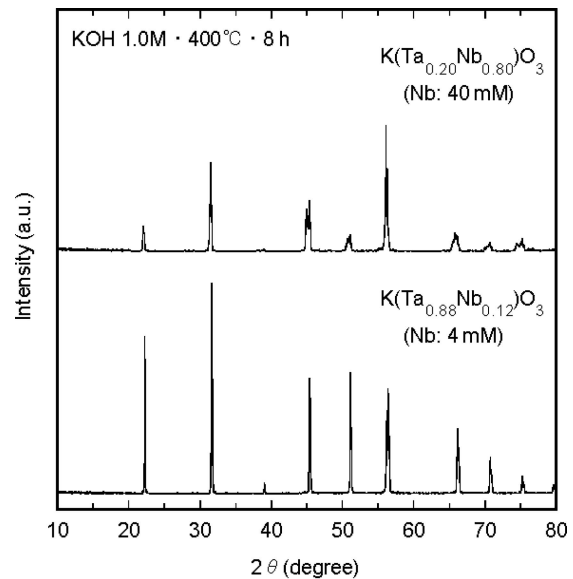


Figure 11 XRD patterns ( $\text{CuK}\alpha$ ) of potassium tantalate niobate films formed at various Nb concentrations. The  $X$  in  $\text{K}(\text{Ta}_{1-X}\text{Nb}_X)\text{O}_3$  is estimated from its lattice volume. Synthesis conditions: 4–40 mM Nb, 1.0 M  $\text{KOH}$ ,  $400^\circ\text{C}$ , 8 h.

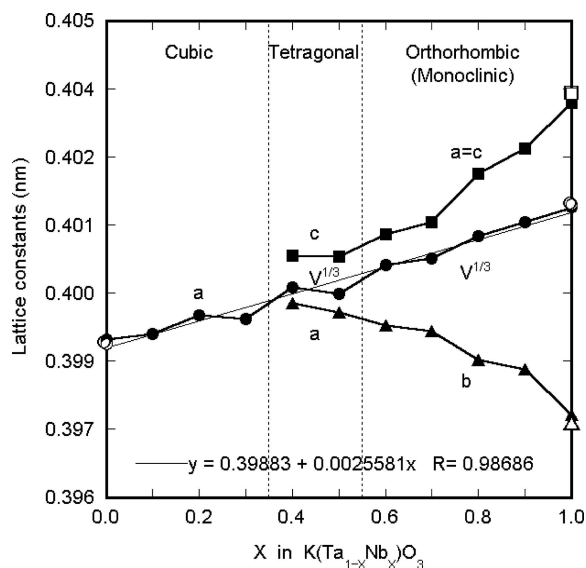


Figure 12 Variation of lattice constants of hydrothermally synthesized  $K(\text{Ta}_{1-x}\text{Nb}_x)\text{O}_3$  perovskite with Nb content  $X$ . Synthesis conditions: 8.0 M KOH, 300°C, 16 h. Open circle at  $X = 0.0$ : PDF #38-1470 ( $\text{KTaO}_3$ ), Open symbols at  $X = 1.0$ : PDF #32-0822 ( $\text{KNbO}_3$ ), —: Regression line for  $V^{1/3}$ .

Fig. 10 depicts the difference in IR spectrum due to OH group at about  $3300\text{ cm}^{-1}$ . Solid-solution films in the system  $\text{KTaO}_3\text{-KNbO}_3$  were also grown on Ta substrates with control of the Nb content in the KOH solutions, as shown in Fig. 11. Fig. 12 demonstrates variation of lattice constants of  $\text{K}(\text{Ta}_{1-x}\text{Nb}_x)\text{O}_3$  perovskite with Nb content  $X$ . The crystal symmetry changed from cubic to tetragonal and further to orthorhombic with increasing  $X$ . These morphotropic phase changes in the hydrothermally synthesized  $\text{K}(\text{Ta}_{1-x}\text{Nb}_x)\text{O}_3$  were nearly the same as those revealed by measuring ferroelectricity of  $\text{K}(\text{Ta}_{1-x}\text{Nb}_x)\text{O}_3$  single crystals grown from melts [18].

## 5. Summary

Thin films of  $\text{ATiO}_3$  ( $A = \text{Ba}, \text{Sr}$ ) were grown by the hydrothermal-electrochemical method with current efficiency of ca. 0.6% to 3.0%. The  $\text{ATiO}_3$  films were found to grow at the film/substrate interface by transport of both A-site and oxygen atoms from the solution to the interface through short-circuit paths. Thin films of  $\text{AZrO}_3$  ( $A = \text{Ba}, \text{Sr}$ ) were also prepared uniformly by the hydrothermal-electrochemical method, applying a potential above ca.

+2 V vs. Ag/AgCl to the Zr substrates. Thin films of  $\text{KMO}_3$  ( $M = \text{Ta}, \text{Nb}$ ) containing only a smaller amount of OH group were formed by the hydrothermal method at 300°C. Thin films of  $\text{K}_2\text{M}_2\text{O}_6$  pyrochlore were formed at lower temperatures and lower KOH concentrations. The morphotropic phase changes in the hydrothermal system  $\text{KTaO}_3\text{-KNbO}_3$  were almost the same as those revealed for  $\text{K}(\text{Ta}, \text{Nb})\text{O}_3$  single crystals grown from melts.

## Acknowledgments

We thank Messrs. Rinsei Ike and Seishiro Goto of Kochi University for their experimental assistance.

## References

1. C. FELDMAN, *Rev. Sci. Instr.* **26** (1955) 463.
2. YU. YA. TOMASHPOLSKI, *Ferroelectrics* **7** (1974) 253.
3. I. H. PRATT, *Proc. IEEE* **59** (1971) 1440.
4. T. SAKUMA, S. YAMAMICHI, S. MATSUBARA, H. YAMAGUCHI and Y. MIYASAKA, *Appl. Phys. Lett.* **57** (1990) 2431.
5. W. A. FEIL, B. W. WESSELS, L. M. TONGE and T. J. MARKS, *J. Appl. Phys.* **67** (1990) 3858.
6. M. HIRATANI, Y. TARUTANI, T. FUKAZAWA, M. OKAMOTO and K. TAKAGI, *Thin Solid Films* **227** (1993) 100.
7. M. YOSHIMURA, S. E. YOO, M. HAYASHI and N. ISHIZAWA, *Jpn. J. Appl. Phys.* **28** (1989) L2007.
8. K. KAJIYOSHI, N. ISHIZAWA and M. YOSHIMURA, *J. Am. Ceram. Soc.* **74** (1991) 369.
9. *Idem.*, *Jpn. J. Appl. Phys.* **30** (1991) L120.
10. K. KAJIYOSHI, K. TOMONO, Y. HAMAJI, T. KASANAMI and M. YOSHIMURA, *J. Am. Ceram. Soc.* **77** (1994) 2889.
11. K. KAJIYOSHI, K. TOMONO, Y. HAMAJI, T. KASANAMI and M. YOSHIMURA, *J. Mater. Res.* **9** (1994) 2109.
12. K. KAJIYOSHI, M. YOSHIMURA, Y. HAMAJI, K. TOMONO and T. KASANAMI, *ibid.*, **11** (1996) 169.
13. K. KAJIYOSHI, K. TOMONO, Y. HAMAJI, T. KASANAMI and M. YOSHIMURA, *J. Am. Ceram. Soc.* **78** (1995) 1521.
14. K. KAJIYOSHI, Y. HAMAJI, K. TOMONO, T. KASANAMI and M. YOSHIMURA, *ibid.*, **79** (1996) 613.
15. K. KAJIYOSHI, Y. SAKABE and M. YOSHIMURA, *Jpn. J. Appl. Phys.* **36** (1997) 1209.
16. K. KAJIYOSHI, R. IKE, A. ONDA and K. YANAGISAWA, Preprints of the 14th Fall Meeting of the Ceramic Society of Japan, Tokyo, Sep. 26–28, 2001, p. 281.
17. *Idem.*, Preprints of the 2003 Annual Meeting of the Ceramic Society of Japan, Tokyo, March 22–24, 2003, p. 48.
18. S. TRIEBWASSER, *Phys. Rev.* **114** (1959) 63.

Received 22 December 2004  
and accepted 11 April 2005